

# One-dimensional ion-beam figuring for grazing-incidence reflective optics

Lin Zhou,<sup>a,b,c</sup> Mourad Idir,<sup>b\*</sup> Nathalie Bouet,<sup>b</sup> Konstantine Kaznatcheev,<sup>b</sup> Lei Huang,<sup>b</sup> Matthew Vescovi,<sup>b</sup> Yifan Dai<sup>a,c</sup> and Shengyi Li<sup>a,c</sup>

<sup>a</sup>College of Mechatronic Engineering and Automation, National University of Defense Technology, 109 Deya Road, Changsha, Hunan 410073, People's Republic of China, <sup>b</sup>NSLS-II, Brookhaven National Laboratory, PO Box 5000, Upton, NY 11973, USA, and <sup>c</sup>Hu'nan Key Laboratory of Ultra-precision Machining Technology, 47 Yanzheng Street, Changsha, Hunan 410073, People's Republic of China. \*Correspondence e-mail: midir@bnl.gov

Received 1 October 2015

Accepted 15 November 2015

Edited by G. E. Ice, Oak Ridge National Laboratory, USA

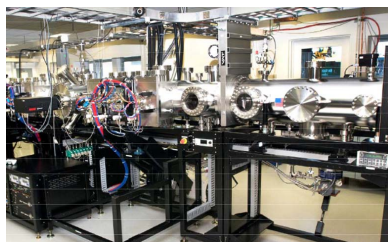
**Keywords:** ion beam figuring; synchrotron optics; one-dimensional.

One-dimensional ion-beam figuring (1D-IBF) can improve grazing-incidence reflective optics, such as Kirkpatrick–Baez mirrors. 1D-IBF requires only one motion degree of freedom, which reduces equipment complexity, resulting in compact and low-cost IBF instrumentation. Furthermore, 1D-IBF is easy to integrate into a single vacuum system with other fabrication processes, such as a thin-film deposition. The NSLS-II Optical Metrology and Fabrication Group has recently integrated the 1D-IBF function into an existing thin-film deposition system by adding an RF ion source to the system. Using a rectangular grid, a 1D removal function needed to perform 1D-IBF has been produced. In this paper, demonstration experiments of the 1D-IBF process are presented on one spherical and two plane samples. The final residual errors on both plane samples are less than 1 nm r.m.s. The surface error on the spherical sample has been successfully reduced by a factor of 12. The results show that the 1D-IBF method is an effective method to process high-precision 1D synchrotron optics.

## 1. Introduction

Numerous synchrotron X-ray applications require high-precision optics (Mimura *et al.*, 2008; Yabashi *et al.*, 2014). For example, Kirkpatrick–Baez mirrors (KB mirrors) used to focus X-ray beams require mirror surface errors to be less than 1 nm r.m.s. in order to focus at the diffraction limit (Yamauchi *et al.*, 2011). With such grazing-incidence optics, figure errors in the scattering plane,  $\varphi$ , blur the image by  $2F_2\varphi$ , where  $F_2$  is the image distance. Out-of-plane figure errors,  $\omega$ , blur the image by  $2\omega F_2 \sin\theta$ , where  $\theta$  is the scattering angle. As a consequence, figure precision in the scattering plane is typically 50 to 1000 times more important than out-of-plane figure errors. Surface roughness is similarly more sensitive to in-plane than to out-of-plane roughness. For this reason, often only the tangential surface error needs to be corrected in order for a mirror to meet application needs.

Ion-beam figuring (IBF) is a powerful technique to fabricate high-precision optics. It has many advantages over traditional optical fabrication processes, such as high determinism, no load force, minimal surface and subsurface damage, and minimal edge effects (Demmler *et al.*, 2010; Franz & Hänsel, 2010; Zhou *et al.*, 2014). IBF is usually a two-dimensional process where the whole optical surface is scanned under the ion beam. However, it is possible to machine grazing-incidence reflective optics, such as the KB mirrors, by only scanning the ion beam along the tangential direction. We called this IBF process one-dimensional IBF (1D-IBF).



© 2016 International Union of Crystallography

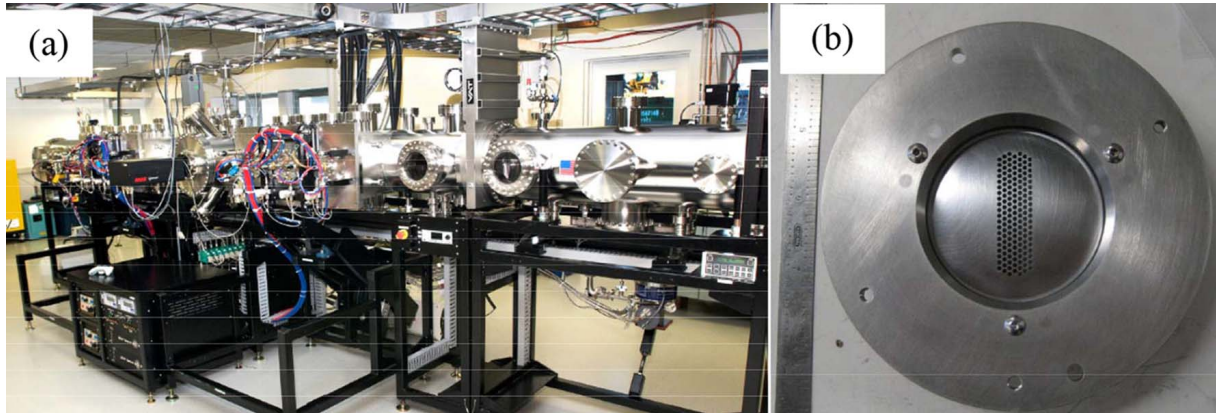


**Figure 1** Equipment used to perform 1D-IBF. (a) BNL self-developed deposition system. (b) Rectangular grid (10 mm × 40 mm) used to generate 1D removal function.

1D-IBF needs only one motion degree of freedom. Comparing with the general IBF system, which needs three or five motion degrees of freedom (Liao *et al.*, 2014a,b), 1D-IBF greatly reduces the complexity of the figuring mechanism, resulting in a compact and low-cost IBF plant. Furthermore, it is easy to integrate 1D-IBF with other fabrication processes, such as a thin-film deposition, into a single vacuum system. For example, the NSLS-II Optical Metrology and Fabrication Group at Brookhaven National Laboratory (BNL) has recently integrated the 1D-IBF function into an existing deposition system which was built to fabricate multilayer Laue lenses for NSLS-II beamlines (Conley *et al.*, 2009). Our experiments in this study were carried out on this modified system.

## 2. Mathematical description

The normal IBF process can be described by a two-dimensional convolution model (Drueding *et al.*, 1995),

$$r(x, y) = p(x, y) \otimes \sigma(x, y) = \int_{-\infty}^{+\infty} \int_{-\infty}^{+\infty} p(x-u, y-v) \sigma(u, v) du dv. \quad (1)$$

Here  $r(x, y)$  is the amount of material removed by the process;  $p(x, y)$  is the removal function of the process,  $\sigma(x, y)$  is the dwell time in the process, and  $\otimes$  stands for the convolution operation.

Similarly, the 1D-IBF process can be described by a 1D convolution model,

$$r(x) = p(x) \otimes \sigma(x) = \int_{-\infty}^{+\infty} p(x-u) \sigma(u) du. \quad (2)$$

Here  $r(x)$  is the amount of material removed by the process along the  $x$ -axis;  $\sigma(x)$  is the dwell time, and  $p(x)$  is the 1D removal function of the process,

$$p(x) = p(x, 0). \quad (3)$$

The calculation of the dwell time  $\sigma$  with the desired removal amount  $r$  and the removal function  $p$  is a deconvolution problem, and many algorithms are applicable (Drueding *et al.*,

1995; Zhou *et al.*, 2007; Liao *et al.*, 2014a). In our study, we use an advanced matrix-based algorithm (Carnal *et al.*, 1992; Zhou *et al.*, 2007) to calculate the dwell time because this algorithm can handle edge data better.

## 3. Experiments

We first calibrated the removal function on a Si mirror. Then, one spherical and two plane mirrors were processed by 1D-IBF.

### 3.1. 1D-IBF process equipment

All 1D-IBF experiments were carried out on the thin-film deposition system (Conley *et al.*, 2009). The vacuum chamber of this system is 23 feet in total length, 14" diameter. Lenses or mirrors are loaded onto a linear-translation stage that moves in one direction back and forth throughout the vacuum system, riding on a stationary base and rail assembly. Besides magnetron sources, which are used to perform thin-film deposition, an RF ion source is installed on the system. This RF ion source is used to clean substrates, and now can be used to perform 1D-IBF. The ion source was modified to generate an approximate 1D removal function by replacing the normal circular accelerate grid with a rectangular grid (10 mm × 40 mm, shown in Fig. 1b).

As a narrow removal function can correct higher spatial frequencies (Zhou *et al.*, 2009), a 10 mm slit is added before the mirrors to obtain a narrower removal function (Fig. 2). An Al slit located at 20 mm from the mirror surface is used in this study.

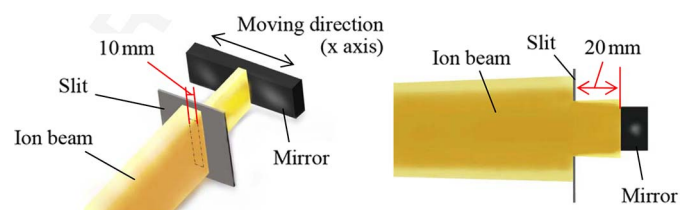


**Figure 2** Layout of our 1D-IBF setup.

### 3.2. Experiment to obtain 1D removal function

Before performing the 1D-IBF process, an experiment was conducted to obtain the removal function. In this experiment, the sample is a 100 mm-diameter plane Si mirror. The ion beam parameters were set to an ion voltage of 800 eV and an ion current of 27 mA. In this test, three footprints of the removal function were etched on the mirror surface at positions  $x = -30$  mm,  $x = 0$ ,  $x = 30$  mm with different etching times of 5 min, 10 min and 15 min, respectively. The surface figure was examined using a Zygo interferometer. The measured surface figure maps before and after the experiment are shown in Figs. 3(a) and 3(b), respectively. The amount of material removed in the test can be calculated from these two figure maps. Fig. 3(c) shows the removal on the interested strip along the  $x$ -axis. This result proves that the removal function is nearly invariant with respect to the  $y$ -coordinate. Fig. 3(d) is the projected map of Fig. 2(c) in the  $xz$  plane. Fig. 3(d) shows very good linearity between the etching time and material removed. The experimental removal function calculated from the data is 14.0 mm wide, with a  $33 \text{ nm min}^{-1}$  removal rate.

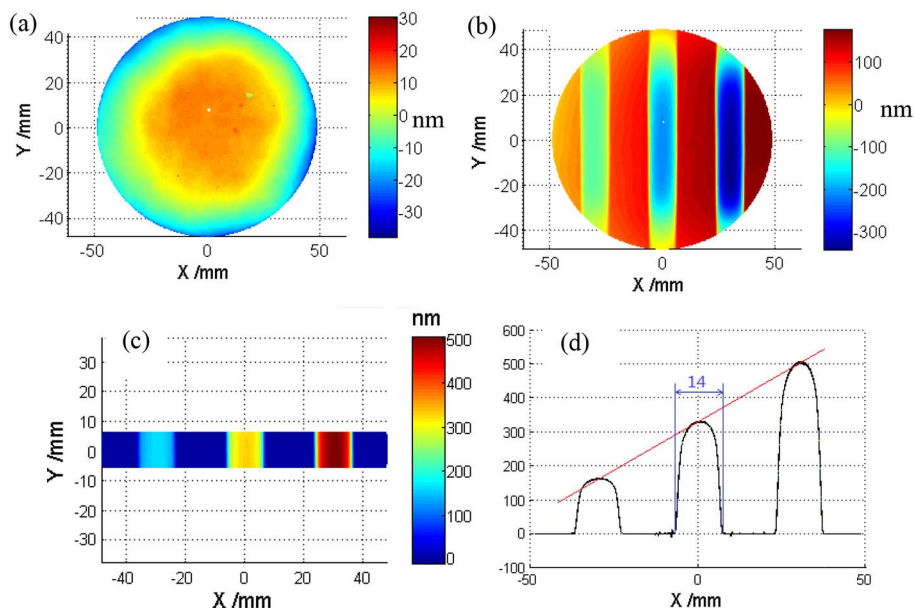


**Figure 3** 1D removal function test results (etching times at  $x = -30$  mm,  $x = 0$ ,  $x = 30$  mm were 5 min, 10 min and 15 min, respectively). (a) Surface figure before experiment. (b) Surface figure after experiment. (c) Removal on the interested strip along the  $x$ -axis. (d) Removal projected in the  $xz$  plane.

### 3.3. 1D-IBF experiments

To perform a 1D-IBF experiment the first step is to measure the surface figure of the optical element. The difference between the measured and the desired figure is then the desired removal amount  $r(x)$ . The dwell time  $\sigma(x)$  can be calculated using equation (2). We calculate the dwell times at intervals of 1 mm. The sum of these dwell times is the desired process time. Since the total time used to move between the points at intervals of 1 mm on a line is much less compared with the process time, we use the point machining mode in our process.

In order to fully demonstrate our 1D-IBF processing capabilities, we performed 1D-IBF experiments on one spherical and two plane samples.

**3.3.1. First 1D-IBF.** The first 1D-IBF experiment was performed on a 96 mm-long plane Si mirror. In this experiment, the surface figure errors were measured using a Zygo interferometer. The measurement results before and after the experiments are shown in Figs. 4(a) and 4(b), respectively. The surface error before the experiment is 24.7 nm peak-to-valley (PV), 5.0 nm RMS. After 4 min of the 1D-IBF process, the surface error was reduced to 5.6 nm PV, 0.6 nm RMS.

**3.3.2. Second 1D-IBF.** The second 1D-IBF experiment was performed on a 90 mm-long plane Si mirror. In both these second set of experiments the surface errors were measured

using a two-dimensional slope measuring system based on a stitching Shack Hartmann optical head (Idir *et al.*, 2014). This new metrology tool offers very good options to perform ion beam figuring finishing; it allows the possibility to perform

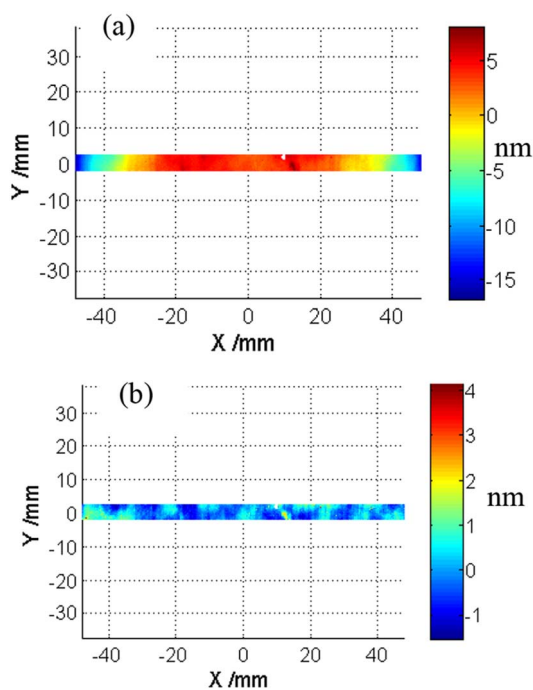


**Figure 4** Results of the first 1D-IBF. (a) Surface error before experiment (24.7 nm PV, 5.0 nm RMS). (b) Surface error after experiment (5.6 nm PV, 0.6 nm RMS).

**Table 1**  
Surface roughness measurement results (units: nm).

	Point number									Average	Std
	1	2	3	4	5	6	7	8	9		
Before 1D-IBF	0.343	0.342	0.340	0.339	0.340	0.337	0.335	0.339	0.338	0.339	0.002
After 1D-IBF	0.342	0.332	0.339	0.330	0.331	0.347	0.330	0.349	0.351	0.339	0.009

measurements of plane and highly curved optics with very high accuracy. The two-dimensional slope measurement results (already converted to height) before and after the experiment are shown in Figs. 5(a) and 5(b), respectively. The surface error before the 1D-IBF experiment is 44.6 nm PV, 14.9 nm RMS. After 9 min of the 1D-IBF process, the surface error was reduced to 4.0 nm PV, 0.72 nm RMS.

The roughness on the surface before and after the experiment was investigated using a Zygo white-light interferometer. We measured nine points along the *x*-axis on the surface. Each point covers an area of 0.351 mm × 0.263 mm and is sampled by 640 × 480 pixels. The measurement results in the RMS of each point, and their averages and standard deviations (Std), are summarized in Table 1. The results show that the roughness after the 1D-IBF process remains the same as the initial roughness 0.339 nm r.m.s.

**3.3.3. Third 1D-IBF.** The third 1D-IBF experiment was performed on an 80 mm-long spherical Si mirror. The two-dimensional slope measurement results (already converted to height) before and after the experiment are shown in Figs. 6(a) and 6(b), respectively. The surface error before the 1D-IBF experiment is 62.9 nm PV, 21.2 nm RMS. After 14 min of the 1D-IBF processing, the surface error was successfully reduced

by a factor of 12. The radius of curvature before and after the 1D-IBF experiment was unchanged at 24.3 m.

#### 4. Conclusion

We have demonstrated 1D-IBF to machine grazing-incidence synchrotron optics, such as KB mirrors. The 1D-IBF process, compared with the conventional three-axis or five-axis motion IBF process, requires only one motion axis. This greatly reduces the complexity of the mechanism, resulting in a compact and low-cost IBF system. Furthermore, it can be easier to integrate with other vacuum processes into a single vacuum system. For example, 1D-IBF and thin-film deposition processes have been successfully built into one vacuum system at BNL.

By employing a rectangular grid on a RF ion source and a second Al slit, a 1D removal function has been produced. Demonstration experiments of 1D-IBF process were performed on one spherical and two plane mirrors. The resulted residual errors on both plane samples are less than 1 nm r.m.s. The surface error on the spherical sample has been successfully reduced by a factor of 12. The results show that the 1D-IBF method is feasible and effective to process high-

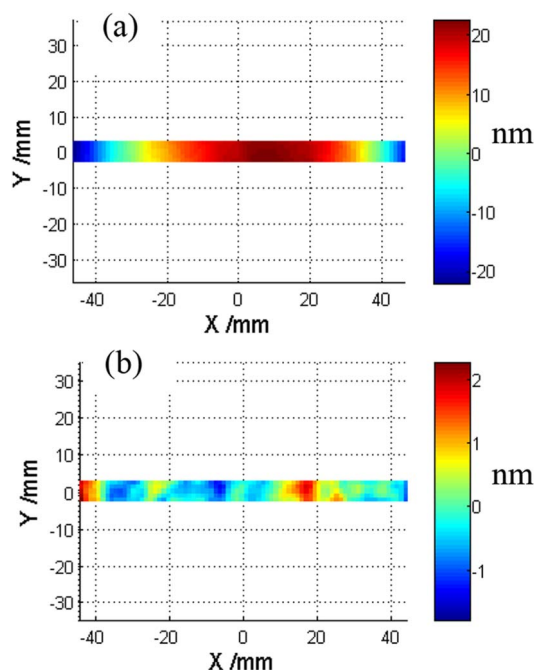


**Figure 5**  
Results of the second 1D-IBF. (a) Surface error before experiment (44.6 nm PV, 14.9 nm RMS). (b) Surface error after experiment (4.0 nm PV, 0.72 nm RMS).

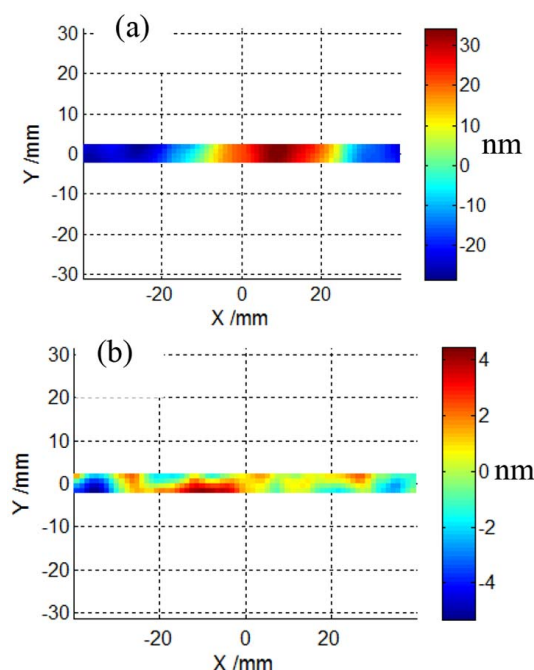


**Figure 6**  
Results of 1D-IBF on spherical 1D optics. (a) Surface error before experiment (62.9 nm PV, 21.2 nm RMS). (b) Surface error after experiment (9.7 nm PV, 1.78 nm RMS).

precision 1D synchrotron optics. This process must be, of course, coupled with high-accuracy metrology.

### Acknowledgements

This work was supported by the US Department of Energy, Office of Science, Office of Basic Energy sciences, under contract No. DE-AC-02-98CH10886. LZ was supported by the Program for New Century Excellent Talents in University (No. NCET-13-0165) and the National Natural Science Foundation of China (No. 91323302). The authors acknowledge Ray Conley for his support during the beginning of this project. The authors greatly appreciate the valuable suggestions and specific comments of the different referees to improve this article.

### References

- Carnal, C., Egert, C. & Hylton, K. W. (1992). *Proc. SPIE*, **1752**, 54–62.
- Conley, R., Bouet, N., Biancarosa, J., Shen, Q., Boas, L., Feraca, J. & Rosenbaum, L. (2009). *Proc. SPIE*, **7448**, 74480U.
- Demmler, M., Zeuner, M., Allenstein, F., Dunger, T., Nestler, M. & Kiontke, S. (2010). *Proc. SPIE*, **7591**, 75910Y.
- Drueding, T., Bifano, T. & Fawcett, S. (1995). *Precis. Eng.* **17**, 10–21.
- Franz, T. & Hänsel, T. (2010). *Proc. SPIE*, **7655**, 765513.
- Idir, M., Kaznatcheev, K., Dovillaire, G., Legrand, J. & Rungsawang, R. (2014). *Opt. Express*, **22**, 2770–2781.
- Liao, W., Dai, Y., Xie, X. & Zhou, L. (2014a). *Appl. Opt.* **53**, 4266–4274.
- Liao, W., Dai, Y., Xie, X. & Zhou, L. (2014b). *Appl. Opt.* **53**, 4275–4281.
- Mimura, H., Morita, S., Kimura, T., Yamakawa, D., Lin, W., Uehara, Y., Matsuyama, S., Yumoto, H., Ohashi, H., Tamasaku, K., Nishino, Y., Yabashi, M., Ishikawa, T., Ohmori, H. & Yamauchi, K. (2008). *Rev. Sci. Instrum.* **79**, 083104.
- Yabashi, M., Tono, K., Mimura, H., Matsuyama, S., Yamauchi, K., Tanaka, T., Tanaka, H., Tamasaku, K., Ohashi, H., Goto, S. & Ishikawa, T. (2014). *J. Synchrotron Rad.* **21**, 976–985.
- Yamauchi, K., Mimura, H., Kimura, T., Yumoto, H., Handa, S., Matsuyama, S., Arima, K., Sano, Y., Yamamura, K., Inagaki, K., Nakamori, H., Kim, J., Tamasaku, K., Nishino, Y., Yabashi, M. & Ishikawa, T. (2011). *J. Phys. Condens. Matter*, **23**, 394206.
- Zhou, L., Dai, Y., Xie, X., Jiao, C. & Li, S. (2007). *Nanotechnol. Precis. Eng.* **5**, 107–112.
- Zhou, L., Dai, Y., Xie, X. & Li, S. (2009). *Sci. China Ser. E*, **52**, 2061–2068.
- Zhou, L., Li, S., Liao, W., Hu, H., Dai, Y. & Xie, X. (2014). *Classical Optics 2014*, OSA Technical Digest (online), paper OM4B. 4.